HHS Public Access

Author manuscript

ACS Nano. Author manuscript; available in PMC 2018 April 09.

Published in final edited form as:

ACS Nano. 2017 July 25; 11(7): 6773–6781. doi:10.1021/acsnano.7b01470.

Covalent Protein Labeling and Improved Single Molecule Optical Properties of Aqueous CdSe/CdS Quantum Dots

Sara M. Wichner[1], **Victor R. Mann**[1,2], **Alexander S. Powers**[2], **Maya A. Segal**[1], **Mustafa Mir**[3], **Jigar Bandaria**[4], **Mark A. DeWitt**[5], **Xavier Darzacq**[3], **Ahmet Yildiz**[3,4,5,*], and **Bruce E. Cohen**[2,*]

[1]Department of Chemistry, University of California at Berkeley, Berkeley CA 94720 USA

[2]Molecular Foundry, Lawrence Berkeley National Laboratory, Berkeley CA 94720 USA

[3]Department of Molecular and Cellular Biology, University of California at Berkeley, Berkeley CA 94720 USA

[4]Department of Physics, University of California at Berkeley, Berkeley CA 94720 USA

[5]Biophysics Graduate Group, University of California at Berkeley, Berkeley CA 94720 USA

Abstract

Semiconductor quantum dots (QDs) have proven to be superior probes for single molecule imaging compared to organic or genetically encoded fluorophores, but they are limited by difficulties in protein targeting, their larger size and on-off blinking. Here, we report compact aqueous CdSe/CdS QDs with significantly improved bioconjugation efficiency and superior single-molecule optical properties. We have synthesized covalent protein labeling ligands (*i.e.*, SNAP tags) that are optimized for nanoparticle use, and QDs functionalized with these ligands label SNAP-tagged proteins ~10-fold more efficiently than existing SNAP ligands. Single-molecule analysis of these QDs shows 99% of time spent in the fluorescent on state, ~4-fold higher quantum efficiency than standard CdSe/ZnS QDs, and 350 million photons detected before photobleaching. Bright signals of these QDs enable us to track the stepping movement of a kinesin motor *in vitro* and the improved labeling efficiency enables tracking of single kinesins in live cells.

Imaging biological systems at the single molecule level reveals the distribution and stochasticity of cellular components present at low copy number and the precise motions of motor proteins and other biomolecular machines. An ongoing challenge is the development of luminescent probes with the brightness, stability, continuous emission, and biocompatibility necessary for single molecule imaging at high spatial and temporal resolution. Semiconductor QDs, such as CdSe/ZnS core/shell heterostructures, are ideal

*Corresponding authors: yildiz@berkeley.edu, becohen@lbl.gov.

COMPETING FINANCIAL INTERESTS

The authors have filed a patent disclosure for the synthetic SNAP ligands.

SUPPORTING INFORMATION

Supporting Information contains tables of nanoparticle sizing details, quantum yields; schemes methods, and characterization for ligand synthesis; figures with QD optical characterization, sizing, photostability, bioconjugation reactions, and cytotoxicity data. The Supporting Information is available free of charge on the ACS Publications website at DOI.

probes because of their narrow emission spectra, high photostability, and large optical cross-sections that lead to enhanced brightness.[1] Use of QDs have enabled tracking the stepping movement of molecular motors, [2–4] transport of cargoes through the nuclear pore complex,[5] and diffusion of receptors in neuronal membranes.[6–8]

Several properties of these QDs have limited their use in single molecule imaging. First, biocompatible QDs are much larger than organic or protein fluorophores.[1, 9–11] There are a limited number of practical methods for targeting QDs to biomolecules of interest, most are non-covalent and not amenable to intracellular or multiplexed labeling, and these may dramatically increase the overall nanoparticle size. While the inorganic QD components are typically <10 nm in diameter,[12, 13] the size of the QD complex is increased by the addition of surface ligands, polymers, or proteins for water dispersibility (Figure 1a and Table S1). Streptavidin (SA) is most often used for bioconjugation, but multiple protein copies on the QD surface increase the complex diameter by >10 nm, [9, 10, 14] and biotinylated antibodies can further increase the diameter of the complex up to 30 nm. Such large complexes may perturb protein function, inhibit labeling in confined or crowded systems, alter tracking kinetics, or present uncertainty in where the nanocrystal sits relative to the protein of interest.

Second, limitations in photon output, photostability, and emission intermittency (*i.e.*, on/off blinking) of CdSe/ZnS QDs interfere with single molecule experiments.[15] Recently a number of high-quality QDs such as quasi-type II CdSe/CdS heterostructures[16–19] and other inorganic nanocrystals[20, 21] have been reported with enhanced photostability and limited or no blinking, advances that have supplanted the use of soluble anti-blinking reagents.[22] These optical advantages are significant but somewhat offset by their larger sizes compared to the CdSe/ZnS QDs commonly used in bioimaging experiments.

In addition to these improved hydrophobic inorganic core/shell structures, much effort has focused on post-synthetic modifications to create small, bright, and stable aqueous QDs. A common method of transferring hydrophobic QD nanocrystals to water involves exchange of hydrophobic surface ligands for polar ones, though recent work has found that removing native ligands alters the nanocrystal surface, leads the loss of surface trap quenchers, and can significantly lower quantum yields and colloidal stability.[23–25] Alternatively, encapsulation of the hydrophobic surface ligands is often done with amphiphilic polymers that preserve optical properties and confer aqueous stability, but increase nanoparticle size.[26–28] New targeting strategies are required to synthesize stable, compact, and bright QD complexes without sacrificing aqueous dispersibility or labeling efficiency.

In this study, we have synthesized CdSe/CdS QDs and functionalized them with hydrophilic covalent bioconjugation reagents optimized for use with inorganic nanocrystals. These QDs have significantly larger optical cross-sections at common excitation wavelengths, enhanced emission and photostability, and reduced blinking compared to standard CdSe/ZnS QDs. Single-molecule analysis of aqueous QDs shows 99% of time spent in the on state, over five-fold greater brightness than commercial QDs, and 350 million photons detected over the life of the QD before photobleaching. These QDs are functionalized with hydrophilic benzylguanine (BG) ligands that covalently modify SNAP tag proteins ~10-fold more

efficiently than existing BG tags. This improved protein labeling efficiency allows live-cell imaging of kinesin motors and dual-color QD labeling of kinesin heads to track its stepping movement *in vitro*.

RESULTS AND DISCUSSION

CdSe QDs require an epitaxial inorganic shell to be useful as bright, stable bioimaging reagents. In type I CdSe/ZnS QDs, the ZnS shell masks surface traps and prevents oxidation of the CdSe core, but its large bandgap keeps it from participating in energy absorption, emission and quantum confinement. In quasi-type II CdSe/CdS heterostructures, the shell participates in energy absorption, while emission occurs only from the core, resulting in QDs with narrow, red-shifted emission and much larger optical cross-sections at shorter wavelengths (*e.g.*, 488 nm), relative to CdSe/ZnS QDs (Figure S1).[29] Based on a recent report of CdSe/CdS QDs with near unity quantum yields,[16] we grew CdSe cores to 2.2 nm and 3.9 nm, as determined by TEM and first exciton peaks.[13] Epitaxial CdS shells (7–8 monolayers, ML) were grown to total diameters of 8.0 ± 1.0 nm and 9.3 ± 0.7 nm (Figure 1b), measured by TEM (Table S1 and Figure 1a) and emission maxima of 587 nm and 626 nm, respectively (Figure 1b). These faceted nanocrystals exhibit symmetric emission spectra with full-width half-maxima of ~25 nm (Figure 1b), enabling us to use QDs that are spectrally close to each other in multicolor imaging applications. Compared to type I CdSe/ZnS QDs with similar emission maxima, the optical cross sections of CdSe/CdS QDs are 3.8 and 1.6-fold greater at 488 nm (Figure S1).

To transfer these QDs from organic to aqueous phases, we wrapped them with low molecular weight amphiphilic polymers (see Methods) to form liposome-like structures around the nanocrystal surface ligands, a procedure shown to preserve quantum efficiency and impart excellent colloidal stability.[26–28] Polymers were synthesized from 2 kDa polyacrylic acid and optimized for non-aggregation with a 3:5:1 ratio of octyl, carboxylate, and ammonium groups (PAOA polymers; Figure S3). Dynamic light scattering (DLS), negative-stain electron microscopy, and fluorescence correlation spectroscopy (FCS) measurements of aqueous QDs show that the combination of surface ligands and polymer adds ~6 nm to the inorganic diameters measured by TEM (Figures 1 and S2), consistent with measurements for other QDs[24] (Table S1). Aqueous CdSe/CdS QDs showed no measurable change in quantum yield compared to their hydrophobic counterparts (Table S3). We obtained sub-10 nm diameters for aqueous CdSe/ZnS QDs and 15 nm for aqueous CdSe/CdS QDs (Figure 1 and Table S1). The size and monodispersity of aqueous CdSe/CdS QDs were unchanged during >4 months of storage at room temperature (Figure S3). In contrast, our attempts to exchange hydrophobic QDs into water by ligand exchange, in which hydrophobic synthetic ligands are replaced by polar ones,[23–24, 30] resulted in QDs with poor colloidal stability that aggregated irreversibly over a matter of days (not shown). While these aqueous QDs are smaller than their polymer-wrapped counterparts, the rapid onset of aggregation makes them unsuitable for many imaging experiments. The addition of a liposome-like structure around the nanocrystals may also impose a low-dielectric barrier to prevent escape of cytotoxic Cd^{2+} ions, and we find that mammalian cells exposed to these QDs show no measurable changes in metabolic activity over a 24-hour exposure (Figure S4).

To characterize these aqueous QDs for single-molecule imaging, we compared emission, blinking, and photostability of comparable CdSe/CdS and CdSe/ZnS QDs under ambient conditions (Figure 2a). Single red CdSe/CdS QDs emit 350 million (detected) photons before photobleaching, ~7-fold more than red CdSe/ZnS QDs (Figure 2b). Surface-immobilized CdSe/CdS QDs were photostable for >20 minutes under continuous 35 W/cm^2 488 nm excitation, and we detected 2×10^5 photons/s on average from individual CdSe/CdS QDs (Figure S5). Single QD emission traces show that these aqueous CdSe/CdS QDs spend 99% of the time in the on state compared to 72% for comparable CdSe/ZnS QDs (Figure 2c). We calculated relative single-molecule quantum yields (QY) based on numbers of photons detected (Figure 2b) and relative optical cross section at 488 nm (Figure S1), and find that the single-particle QY of the 626-nm CdSe/CdS QDs is 4-fold higher than that of comparable CdSe/ZnS QDs (Table S2). This is significantly larger than ensemble QY differences measured at lower excitation powers (Table S3).

To optimize the labeling efficiency without compromising the nanoparticle size, we functionalized the QD surface with O^6-benzylguanine (BG) SNAP tags.[31] The SNAP labeling pair consists of a 20 kDa alkyltransferase fusion protein and BG ligands that covalently react with the enzyme.[32] Covalent attachment of the BG ligand to QD polymer amines led to a marginal increase (<1 nm) in nanoparticle size (Figure 1e). To measure the efficiency of protein labeling with BG-coated QDs, we inserted a SNAP-tag to the N-terminus of a truncated version (K560) of human kinesin-1, a dimeric motor that processively takes 8 nm steps towards the plus-end of microtubules (Figure 3).[33] Kinesin walks by alternating stepping of its two motor domain heads in a hand-over-hand (HoH) motility.[2] The stepping movement of a single head of a kinesin dimer has been studied extensively by labeling with SA-coated QDs[4] or gold nanoparticles,[34] although these large (>20 nm diameter) probes may interfere with kinesin motility. We reasoned that our compact BG-coated QDs enable higher labeling efficiency with minimal perturbation to kinesin motility.

The SNAP-K560-GFP construct was purified (see Methods), labeled with excess QDs, and the motility of individual motors along surface-immobilized microtubules was monitored using total internal reflection fluorescence (TIRF) microscopy (Figure 3a and Video S1). SNAP labeling efficiency has been reported to be as high as 90% with organic dyes,[35] but our initial attempts to label kinesin protein SNAP-K560-GFP on its head with BG-functionalized QDs showed efficiencies under 3% (Figure 3). Addition of co-solvent glycerol, which is commonly used to improve the solubility of hydrophobic ligands without compromising protein function, improved labeling marginally, and we found labeling efficiency decreased over time from the SNAP-QD synthesis. This suggested that the hydrophobic ligand becomes increasingly unreactive, possibly by partitioning to the nonpolar layer surrounding the QD and becoming inaccessible to the enzyme. Consistent with this poor SNAP tag reactivity, all attempts to label with hydrophobic Halotag ligands[36] with QDs were also unsuccessful (not shown).

To improve labeling, we synthesized two SNAP amine-reactive succinimidyl esters containing either an extended hydrophilic linker (BG-PEG$_5$-SE) or a charged sulfonate group (sulfoBG-SE) (Figures 3c and Scheme S1). These BG ligands were covalently

attached to QD surfaces *via* polymer amines, leading to a small increase in total diameter, measured by DLS (Figure 1e and Table S1). Labeling efficiency of kinesin by BG-coated QDs for both of these ligands were significantly improved, with sulfoBG QDs showing an optimized efficiency of 34% (Figure 3d). While the flexible PEG linker improves labeling efficiency by presumably distancing the ligand from the nanoparticle surface, this distance and flexibility may introduce uncertainty about where the QD sits relative to the bound protein of interest. To avoid this uncertainty, we used the smaller sulfoBG ligands, with 10 atoms between attachment points (Figure 3c), in all following bioimaging studies. First, we used these QDs to monitor the stepping movement of SNAP-K560-GFP motors labeled with single sulfoBG QDs along microtubules *in vitro* at 7.5 μM ATP (Video S2). Individual fluorescent spots were tracked at 30 Hz with 1 nm precision (Figure 3e). The step analysis revealed that a kinesin head takes 16 nm steps at limited ATP concentration, in agreement with previous studies and demonstrating that labeling with these QDs does not measurably alter kinesin motions.[2, 34]

To test this covalent QDs labeling within live cells, we microinjected red sulfoBG QDs into HeLa cells expressing SNAP-tagged kinesin-1 (Figure 4a). Microinjection is useful for avoiding the bright puncta associated with endocytosis, which can persist for hours even with the best nanoparticle delivery methods,[37] and which overwhelm signals from single QDs. For this assay, we extended the neck-linker region of kinesin with 7 Gly-Ser repeats (SNAP-K560$_{14GS}$-GFP) to facilitate microtubule binding in a two-heads bound state in the absence of a cargo.[4, 38] Within 2 minutes after injection, we observed diffraction-limited spots moving processively along microtubules at 88 ± 35 nm/s (mean ± s.e.m., N = 7, Figure 4b), comparable to the velocity (129 ± 21 nm/s, N = 36) of this construct at saturating ATP *in vitro* (Video S3).[4] This processive movement of injected QDs was not observed in cells that do not express SNAP-K560$_{14GS}$-GFP (N_{cells} = 10). These results show that sulfoBG QDs are able to rapidly label kinesin motors in live cells without perturbing their complex dynamic properties.

Since the introduction of aqueous QDs for bioimaging, a sustained effort has been made to improve their properties as cellular imaging probes. These improvements have included suppression of on-off blinking, reductions in overall nanoparticle size, and improved aqueous passivation for bioconjugation and added stability in cellular environments, but often these improvements have been at odds with one another. For example, large CdS shells virtually eliminate blinking[16–19] and large aqueous passivation layers improve chemical stability,[26–28] but both add substantially to overall nanoparticle size. Conversely, exchange of native hydrophobic for small hydrophilic ligands reduces QD size and introduces handles for bioconjugation, but removal of native ligands can reconfigure the nanocrystal surface in ways that degrade both brightness and colloidal stability.[23–25] Other studies have found that reagents commonly used in bioconjugation, including Cu(I)[39] and diimide coupling reagents,[40] can fully quench QDs. SA-biotin remains the most common method for QD targeting, even though SA adds >10 nm to QD diameter[9, 12] and may be conjugated at the QD surface in conformations unable to bind biotin.[10]

Here, we build on this work to synthesize compact aqueous CdSe/CdS QDs with hydrophilic bioconjugation ligands and demonstrate that they improve upon conventional QDs in all of

these respects. SNAP tags have been widely adopted for protein-specific labeling in cell biology,[36, 41–42] and we find that addition of hydrophilic groups to the SNAP ligand enables them to be functional on QD surfaces, as well as substantially reduces nanoparticle size compared to other targeting strategies. Compared to protein-coated nanoparticles, compact size of these QDs improve labeling in confined or crowded systems (*e.g.*, the synapse[6] or nuclear pore complex[5]) and reduce perturbation to kinetics and function of labeled proteins. A nearly 10-fold higher labeling efficiency of sulfoBG than the hydrophobic ligand suggests experiments requiring dual labeling of a multimeric protein[43] to improve by two orders of magnitude. This approach is also orthogonal to other protein-based targeting pairs (*e.g.*, CLIP tags[36]) as well as abiotic coupling reactions,[39] which may enable specific multicolor labeling in or on cells.

Antibody-based QD targeting has been effective for non-covalent labeling of extracellular protein domains, and advances in antibody engineering have produced small immuno-QD complexes for cell imaging.[44–45] SNAP-based covalent targeting methods extend QD imaging to intracellular targets in live cells, targets for which high-affinity antibodies cannot be produced, and experiments requiring an irreversible bond between QD and target. For characterization of motor protein motions as in Figures 3 and 4, the covalent labeling is critical to distinguish the motor protein dissociating from the cytoskeleton[2, 4] versus the QD dissociating from the motor protein. Covalent labeling offers confidence for these and other long-term tracking studies that will leverage the exceptional optical stability of these QDs.

Single particle imaging demands that QDs probes have exceptional stability, particularly for long-term tracking or use within live cells. Exchange of native ligands for hydrophilic thiols or other coordinating ligands produces functional QDs with small passivation shells, which is an advantage for many imaging applications.[30, 46] Our attempts to shrink the QD complex by ligand exchange have been unsuccessful in producing single molecule probes, and we have found that retention of native ligands within a liposome-like structure is essential for the brightness, chemical stability, and photostability required for single molecule experiments. Monovalent ligands are rapidly displaced by other ligands,[47] such as the thiols found in the cytosol, and are prone to photooxidation under the high photon flux required for single-molecule imaging.[48] Here we demonstrate tracking kinesin continuously with sub-nanometer localization accuracy over minutes to hours, and are also able to track single kinesins in live cells. The live-cell experiments are also facilitated by the high labeling efficiencies of sulfoBG (Figure 3d), as it would be difficult to identify QD-kinesin complexes if the vast majority of the SNAP-QDs within a cell were unbound.

The use of high-quality type II CdSe/CdS QDs[9] and a water transfer strategy that preserves their superior optical properties yields aqueous QDs with significantly better single-particle on-state fractions, quantum yields, photon output, and photostability compared to other aqueous QDs. This improvement in total emission may enable bioimaging with improved localization accuracy,[6] longer tracking times,[7] highly localized biosensing, multicolor super-resolution imaging,[49] and other experiments requiring ultrasensitive probes.

METHODS

Synthesis of CdSe cores

CdSe cores were synthesized based on the method of Bawendi,[10] with minor modifications. In an Ar glovebox, 58 mg of Se powder (Aldrich, 99.99% trace metal basis) was added to 0.36 g of trioctylphosphine (TOP, Aldrich, 97%) in a glass vial and stirred overnight, yielding TOP-Se as a clear, colorless solution. On a Schlenk line, 60 mg of CdO (Aldrich, 99.99% trace metal basis, 0.47 mmol), 0.28 g of octadecylphosphonic acid (ODPA, 0.84 mmol), and 3.0 g of TOP oxide were combined in a 50-mL flask fitted with a condenser and temperature probe. The flask was heated under N_2 to 150 °C and stirred under vacuum for 1 hr. The solids melted at 70 °C. The flask was purged with N_2 and heated to 320 °C until the Cd had complexed with the ODPA to become clear and colorless. TOP (1.50 g) was injected into the flask drop-wise and the temperature was then raised to 370 °C. The TOP-Se precursor was then rapidly injected, and growth time was controlled to achieve the desired particle size. The flask was cooled with air and then submerged in an ice bath after the temperature cooled below 300 °C. At 110 °C, 3 mL of cold toluene was injected. The final reaction solution was removed and the total volume of the solution was diluted with toluene to 15 mL. The particles were then precipitated with 15 mL of acetone and centrifuged at 4000 × *g* for 5 min. The pellet was dispersed in a minimum of $CHCl_3$, precipitated with 10 mL of acetone, centrifuged at 4000 × *g* for 5 min, dispersed in a minimum of hexane (~1 mL), and precipitated with acetone again. These cores were dispersed in 5 mL of hexane and stored in a glovebox.

Synthesis of core-shell CdSe/CdS nanoparticles

Stock solutions of 0.1 M Cd oleate in octadecene (ODE) and 0.1 M octanethiol in ODE were prepared in a glovebox. On a Schlenk line, 5 mL of ODE was placed in a 3-neck flask under N_2 and 100 nmol of CdSe core nanocrystals in hexane were injected. Solvent was removed under vacuum at room temperature and then at 120 °C for 20 min. The reaction was purged with N_2 and the glovebox solutions containing 6 mL of 0.1 M Cd oleate/ODE and 6 mL of 0.1 M octanethiol/ODE were injected at 310 °C *via* 2 syringe pumps over 2 hr. After injection, 1 mL of oleic acid was quickly injected and the reaction maintained at 310 °C for 1 hr. The reaction was cooled with air, the nanocrystals cleaned by repeated precipitation as above, and the nanocrystals dispersed in 5 mL of hexane with 1% oleic acid (v/v) for storage under ambient conditions.

Passivation of QDs by PAOA amphiphilic copolymer

CdSe/CdS QD core/shells with emission maxima of 587 nm and 626 nm were synthesized as described above and dispersed in toluene to 17 μM and 8 μM, respectively and stored in 1% oleic acid to prevent aggregation. CdSe/ZnS QD core/shells with emission maxima of 585 nm and 630 nm (Ocean Nanotech) were dispersed in toluene to 12 μM and 7 μM, respectively. Concentrations were determined by first exciton peak absorbance.[13] For aqueous dispersion, 11 mg (3.4 μmol, 5000-fold molar excess over QDs) of poly(acrylic acid)-*co*-poly(*n*-octylacrylamide)-*co*-poly(2-aminoethylacrylamide) random amphiphilic copolymer (PAOA; see SI Methods) was dissolved in 1 mL of MeOH and 19 mL of $CHCl_3$. QDs in toluene (*e.g.*, 40 μL of 17 μM 587-nm CdSe/CdS QDs, 0.68 nmol) were added with

stirring, and the solvents were removed under a gentle stream of N_2 overnight. The dry QD/polymer residue was then resuspended in 15 mL of 200 mM borate buffer, pH 9.0. This suspension was sonicated for 15 min, heated in an 80 °C water bath for 30 min, slowly cooled to room temperature, and then sonicated for 15 min. Excess polymer was removed by spin dialysis (Amicon Ultra-15, 50 kDa MWCO), washing with 3 × 10 mL of 0.1M HEPES, pH 8.0. The retentate was diluted to 500 μL with HEPES buffer and centrifuged at 16100 × *g* for 5 min to remove residual polymer. Aggregates were removed by centrifuging the QD solution through a large pore spin column (Pall Nanosep, 300 kDa MWCO). Aqueous QD dispersions were stored under ambient conditions.

Synthesis of sulfoBG QDs

Polymer-wrapped QDs (1.4 μM, 50 μL) in 0.1M HEPES, pH 8.0, were mixed with 3 μL of 10 mM DMSO solutions of both sulfoBG-GLA-SE and methoxy-PEG_4-SE and vortexed well. After 1 hr, the volume was increased to 500 μL with BRB80 buffer (80 mM PIPES, 2 mM EGTA, 1 mM $MgCl_2$, pH 6.8) and excess SE reagents were removed *via* spin dialysis (Amicon Ultra, 50 kDa MWCO), washing 2 additional times with BRB80. The functionalized QDs were stored at room temperature in the dark to reduce the likelihood of photooxidation of the BG ligands.

To detect SNAP ligands on the QD surface, excess BG ligand was removed using FPLC size exclusion chromatography (GE Akta; Superdex 12/200) and the QD-BG absorbance spectra collected from 250 nm to 800 nm. Spectra for aqueous QDs with and without BG ligands were normalized to the first exciton peak and subtracted to obtain the spectrum of surface BG. The extinction coefficient of benzylguanine at 280 nm (7100 M^{-1} cm^{-1})[35] was used to calculate BG concentrations.

Cloning, protein expression, and purification

A truncated version of human kinesin-1 (K560) was used to study kinesin motility. K560 was fused with GFP and a hexahistidine tag at the C-terminus. A SNAP-tag was fused to the N-terminal head domain for specific labeling of kinesin by QDs. The kinesin neck-linker was extended by seven glycine-serine repeats ($K560_{14GS}$).[4] The constructs were expressed in *E. coli* and purified using a Ni^{+2} gravity column. Inactive motors were removed using an MT bind-and-release assay and stored in BRB80 at −80°C.

TIRF microscopy

A home-built objective-type total internal reflection fluorescence (TIRF) setup consisting of a Nikon Ti-E Eclipse inverted fluorescence microscope with Perfect Focusing System and a 100× 1.49 Plan Apo oil immersion objective (Nikon) was used for *in vitro* microscopy experiments. GFP and QDs were excited by a 488 nm solid-state laser (Coherent). For two-color experiments, fluorescence signal was split into two channels using an Optosplit II image splitter (Cairn Instruments), equipped with appropriate filters for GFP and QD fluorescence (Semrock). The fluorescence signal was recorded with an electron-multiplied charge-coupled device (EM-CCD) camera (Ixon EM+, 512×512 pixels, Andor) with 160 nm effective pixel size. Movies were acquired at 10 Hz frame rate.

Single-QD optical characterization

Aqueous CdSe/ZnS and CdSe/CdS QDs were dispersed in BRB80 and introduced to a flow chamber. Excess QD was washed away with 45 μL of BRB80. TIRF imaging was performed at various power densities of 488 nm excitation. Individual QDs were identified by blinking behavior and luminescence intensity histograms were compiled from ~20–50 individual particles for each QD type. The emission from QDs under 100 W/cm^2 illumination was collected for 30 minutes to measure the illumination time until photobleaching and the total number of photons detected before bleaching. Relative intensities of 626 CdSe/ZnS and 630 CdSe/CdS were compared under 35 W/cm^2 excitation. ON and OFF thresholds for blinking were determined from the histogram of individual QD intensity traces.

For determination of relative QY of the QDs, absorbance ratios of CdSe/CdS to CdSe/ZnS at 488 nm were measured using UV/Vis spectroscopy. Average numbers of photons emitted by single QDs under TIRF excitation was used to calculate emission ratios of CdSe/CdS to CdSe/ZnS. The emission ratio was divided by the absorption ratio to calculate relative QY.

Kinesin motility assays

Assays were performed using sea urchin axonemes nonspecifically adsorbed to glass coverslips. The coverslip/axoneme surface was passivated with BRBC (BRB80 supplemented with 1 mg/mL casein and 0.4 mM TCEP) to prevent nonspecific adsorption of the motors and QDs. For single-color tracking experiments, kinesin motors (~1 μg/mL) were incubated with 1 μl of 100 nM 630 nm sulfoBG QDs for 12 min at room temperature. Labeled motor was flowed into the chamber, and the motor density on axonemes was evaluated by detecting the GFP fluorescence. After 2 min of incubation, unbound motors were washed away three times with 15 μL of BRBC. Movies were recorded in the presence of BRBC containing 7.5 μM ATP and an ATP regeneration system (2 mM phospoenolpyruvate and 0.1 mg/mL pyruvate kinase). For single-color experiments, the exposure time was 70 ms per frame. ATP concentration was adjusted for each motor to reduce the stepping rate to 0.1 steps per frame.

Determination of SNAP labeling efficiencies

SNAP-K560$_{14GS}$-GFP (1 μL, ~1 μg/mL) were labeled in the presence of BG-, BG-PEG$_5$- or sulfoBG-functionalized QDs (1 μL, ~100 nM). These labeled motors were diluted to single-molecule concentrations and allowed to decorate axonemes adsorbed to a coverslip in a microscope flow chamber. Motility of individual motors was recorded at 1 mM ATP and 1 s exposure time per frame. The labeling ratio was determined by dividing the number of processively moving spots in the QD channel by the number of processively moving spots in the GFP channel. To prevent crosslinking of multiple motors due to the multivalency of QDs, axonemes were sparsely decorated with kinesin motors and the excess motor was washed away before QDs were introduced to the flow chamber, as a control. Labeling of the motors on axonemes did not result in a significant difference in labeling efficiency and single molecule motility.

Microinjection and live-cell imaging

SNAP-K560$_{14GS}$-GFP was subcloned into the pEGFP-C1 vector. For transient expression of the construct in HeLa cells, the cells were plated at 70% confluency on Mattek plates 12 hours before transfection. Transfection was carried out with Lipofectamine 2000 (Invitrogen) following the manufacturer protocol.

SulfoBG 626-nm CdSe/CdS QDs were diluted to ~10 nM with 0.2 μm-filtered 1 mg/mL BSA, sonicated for 5 min, and centrifuged at 6000 × *g* for 5 min. The resulting supernatant (2 μL) was back-pipetted into Femtotips II needles, which were loaded onto a microinjection system consisting of a Femtojet controller (Eppendorf). The injection parameters were 8.8 kPa, 0.3 sec injection time, and 2.9 kPa compensation pressure. Cells showing strong expression of GFP kinesin were selected for microinjection. Images were collected using a Nikon Eclipse Ti with a Nikon Apo TIRF 100×/1.49 NA oil-immersion objective microscope in TIRF mode using 532 nm excitation from a solid-state white light lamp (Lumencor) at 20 ms time resolution using an Andor iXon Ultra EMCCD camera.

Data Analysis

Kymographs of moving fluorescent spots were analyzed using ImageJ. Diffusive motors or the motors that walked shorter than 2 pixels (320 nm) on a microtubule were excluded from data analysis. Individual spots were tracked using a 2D Gaussian algorithm written in Matlab. The traces were fitted with a custom Matlab script that utilizes a Schwartz Information Criterion to detect steps. [50] Mean-square displacement (MSD) of individual spots were fitted to a polynomial function, $\langle\chi^2\rangle = 4Dt^{\alpha}$, where D is the diffusion constant. The first ($\alpha = 1$) and second ($\alpha = 2$) order polynomial fits represent Brownian motion and unidirectional transport, respectively.

Supplementary Material

Refer to Web version on PubMed Central for supplementary material.

Acknowledgments

We thank C. Tajon, P. Qin, and S. Can for helpful discussions and technical assistance, and W. Huang for help with fluorescence correlation microscopy. This work has been supported by NIH (GM094522 and GM118773 to AY; NS096317 to BC), NSF (MCB-1617028, AY), Miller Institute (AY), and California Institute for Regenerative Medicine (CIRM, LA1-08013 to X.D.). Work at the Molecular Foundry was supported by the Director, Office of Science, Office of Basic Energy Sciences, Division of Materials Sciences and Engineering, of the U.S. Department of Energy under Contract No. DE-AC02-05CH11231.

References

1. Bruchez M, Moronne M, Gin P, Weiss S, Alivisatos AP. Semiconductor Nanocrystals as Fluorescent Biological Labels. Science. 1998; 281:2013–2016. [PubMed: 9748157]
2. Yildiz A, Tomishige M, Vale RD, Selvin PR. Kinesin Walks Hand-Over-Hand. Science. 2004; 303:676–8. [PubMed: 14684828]
3. Warshaw DM, Kennedy GG, Work SS, Krementsova EB, Beck S, Trybus KM. Differential Labeling of Myosin V Heads with Quantum Dots Allows Direct Visualization of Hand-Over-Hand Processivity. Biophys J. 2005; 88:L30–32. [PubMed: 15764654]

4. Yildiz A, Tomishige M, Gennerich A, Vale RD. Intramolecular Strain Coordinates Kinesin Stepping Behavior Along Microtubules. Cell. 2008; 134:1030–41. [PubMed: 18805095]
5. Lowe AR, Siegel JJ, Kalab P, Siu M, Weis K, Liphardt JT. Selectivity Mechanism of the Nuclear Pore Complex Characterized by Single Cargo Tracking. Nature. 2010; 467:600–603. [PubMed: 20811366]
6. Dahan M, Levi S, Luccardini C, Rostaing P, Riveau B, Triller A. Diffusion Dynamics of Glycine Receptors Revealed by Single-Quantum Dot Tracking. Science. 2003; 302:442–445. [PubMed: 14564008]
7. Cai E, Ge PH, Lee SH, Jeyifous O, Wang Y, Liu YX, Wilson KM, Lim SJ, Baird MA, Stone JE, Lee KY, Davidson MW, Chung HJ, Schulten K, Smith AM, Green WN, Selvin PR. Stable Small Quantum Dots for Synaptic Receptor Tracking on Live Neurons. Angew Chem Int Edit. 2014; 53:12484–12488.
8. Groc L, Lafourcade M, Heine M, Renner M, Racine V, Sibarita JB, Lounis B, Choquet D, Cognet L. Surface Trafficking of Neurotransmitter Receptor: Comparison Between Single-Molecule/Quantum Dot Strategies. J Neurosci. 2007; 27:12433–12437. [PubMed: 18003820]
9. Howarth M, Liu W, Puthenveetil S, Zheng Y, Marshall LF, Schmidt MM, Wittrup KD, Bawendi MG, Ting AY. Monovalent, Reduced-Size Quantum Dots for Imaging Receptors on Living Cells. Nat Methods. 2008; 5:397–399. [PubMed: 18425138]
10. Yao J, Larson DR, Vishwasrao HD, Zipfel WR, Webb WW. Blinking and Nonradiant Dark Fraction of Water-Soluble Quantum Dots in Aqueous Solution. Proc Natl Acad Sci US A. 2005; 102:14284–14289.
11. Cohen BE. Biological Imaging: Beyond Fluorescence. Nature. 2010; 467:407–408. [PubMed: 20864989]
12. Dabbousi BO, RodriguezViejo J, Mikulec FV, Heine JR, Mattoussi H, Ober R, Jensen KF, Bawendi MG. (CdSe)ZnS Core-Shell Quantum Dots: Synthesis and Characterization of a Size Series of Highly Luminescent Nanocrystallites. J Phys Chem B. 1997; 101:9463–9475.
13. Jasieniak J, Smith L, van Embden J, Mulvaney P, Califano M. Re-examination of the Size-Dependent Absorption Properties of CdSe Quantum Dots. J Phys Chem C. 2009; 113:19468–19474.
14. Hendrickson WA, Pahler A, Smith JL, Satow Y, Merritt EA, Phizackerley RP. Crystal-Structure of Core Streptavidin Determined from Multiwavelength Anomalous Diffraction of Synchrotron Radiation. Proc Natl Acad Sci US A. 1989; 86:2190–2194.
15. Nirmal M, Dabbousi BO, Bawendi MG, Macklin JJ, Trautman JK, Harris TD, Brus LE. Fluorescence Intermittency in Single Cadmium Selenide Nanocrystals. Nature. 1996; 383:802–804.
16. Chen O, Zhao J, Chauhan VP, Cui J, Wong C, Harris DK, Wei H, Han HS, Fukumura D, Jain RK, Bawendi MG. Compact High-Quality CdSe-CdS Core-Shell Nanocrystals with Narrow Emission Linewidths and Suppressed Blinking. Nat Mat. 2013; 12:445–451.
17. Chen Y, Vela J, Htoon H, Casson JL, Werder DJ, Bussian DA, Klimov VI, Hollingsworth JA. “Giant” Multishell CdSe Nanocrystal Quantum Dots with Suppressed Blinking. J Am Chem Soc. 2008; 130:5026–5027. [PubMed: 18355011]
18. Mahler B, Spinicelli P, Buil S, Quelin X, Hermier JP, Dubertret B. Towards Non-Blinking Colloidal Quantum Dots. Nat Mat. 2008; 7:659–664.
19. Dennis AM, Mangum BD, Piryatinski A, Park YS, Hannah DC, Casson JL, Williams DJ, Schaller RD, Htoon H, Hollingsworth JA. Suppressed Blinking and Auger Recombination in Near-Infrared Type-II InP/CdS Nanocrystal Quantum Dots. Nano Lett. 2012; 12:5545–5551. [PubMed: 23030497]
20. Wu S, Han G, Milliron DJ, Aloni S, Altoe V, Talapin DV, Cohen BE, Schuck PJ. Non-Blinking and Photostable Upconverted Luminescence from Single Lanthanide-Doped Nanocrystals. Proc Natl Acad Sci US A. 2009; 106:10917–10921.
21. Chan EM, Levy ES, Cohen BE. Rationally Designed Energy Transfer in Upconverting Nanoparticles. Adv Mat. 2015; 27:5753–5761.
22. Hohng S, Ha T. Near-Complete Suppression of Quantum Dot Blinking in Ambient Conditions. J Am Chem Soc. 2004; 126:1324–1325. [PubMed: 14759174]

23. Anderson NC, Hendricks MP, Choi JJ, Owen JS. Ligand Exchange and the Stoichiometry of Metal Chalcogenide Nanocrystals: Spectroscopic Observation of Facile Metal-Carboxylate Displacement and Binding. J Am Chem Soc. 2013; 135:18536–18548. [PubMed: 24199846]
24. Caldwell MA, Albers AE, Levy SC, Pick TE, Cohen BE, Helms BA, Milliron DJ. Driving Oxygen Coordinated Ligand Exchange at Nanocrystal Surfaces Using Trialkylsilylated Chalcogenides. Chem Comm. 2011; 47:556–558. [PubMed: 21103582]
25. Owen JS, Park J, Trudeau PE, Alivisatos AP. Reaction Chemistry and Ligand Exchange at Cadmium-Selenide Nanocrystal Surfaces. J Am Chem Soc. 2008; 130:12279–12281. [PubMed: 18722426]
26. Albers AE, Chan EM, McBride PM, Ajo-Franklin CM, Cohen BE, Helms BA. Dual-Emitting Quantum Dot/Quantum Rod-Based Nanothermometers with Enhanced Response and Sensitivity in Live Cells. J Am Chem Soc. 2012; 134:9565–9568. [PubMed: 22642769]
27. Anderson RE, Chan WCW. Systematic Investigation of Preparing Biocompatible, Single, and Small ZnS-Capped CdSe Quantum Dots with Amphiphilic Polymers. ACS Nano. 2008; 2:1341–1352. [PubMed: 19206301]
28. Pellegrino T, Manna L, Kudera S, Liedl T, Koktysh D, Rogach AL, Keller S, Radler J, Natile G, Parak WJ. Hydrophobic Nanocrystals Coated With an Amphiphilic Polymer Shell: A General Route to Water Soluble Nanocrystals. Nano Lett. 2004; 4:703–707.
29. Talapin DV, Nelson JH, Shevchenko EV, Aloni S, Sadtler B, Alivisatos AP. Seeded Growth of Highly Luminescent CdSe/CdS Nanoheterostructures with Rod and Tetrapod Morphologies. Nano Lett. 2007; 7:2951–2959. [PubMed: 17845068]
30. Ohyanagi T, Shima T, Okada Y, Tsukasaki Y, Komatsuzaki A, Tsuboi S, Jin T. Compact and Stable SNAP Ligand-Conjugated Quantum Dots as a Fluorescent Probe for Single-Molecule Imaging of Dynein Motor Protein. Chem Comm. 2015; 51:14836–14839. [PubMed: 26267231]
31. Keppler A, Gendreizig S, Gronemeyer T, Pick H, Vogel H, Johnsson K. A General Method for the Covalent Labeling of Fusion Proteins with Small Molecules *In Vivo*. Nat Biotech. 2003; 21:86–89.
32. Gautier A, Juillerat A, Heinis C, Correa IR, Kindermann M, Beaufils F, Johnsson K. An Engineered Protein Tag for Multiprotein Labeling in Living Cells. Chemistry & Biology. 2008; 15:128–136. [PubMed: 18291317]
33. Svoboda K, Schmidt CF, Schnapp BJ, Block SM. Direct Observation of Kinesin Stepping by Optical Trapping Interferometry. Nature. 1993; 365:721–727. [PubMed: 8413650]
34. Mickolajczyk KJ, Deffenbaugh NC, Arroyo JO, Andrecka J, Kukura P, Hancock WO. Kinetics of Nucleotide-Dependent Structural Transitions in the Kinesin-1 Hydrolysis Dycle. Proc Natl Acad Sci US A. 2015; 112:E7186–E7193.
35. Juillerat A, Gronemeyer T, Keppler A, Gendreizig S, Pick H, Vogel H, Johnsson K. Directed Evolution of *O*-6-alkylguanine-DNA Alkyltransferase for Efficient Labeling of Fusion Proteins with Small Molecules *In Vivo*. Chemistry & Biology. 2003; 10:313–317. [PubMed: 12725859]
36. Stagge F, Mitronova GY, Belov VN, Wurm CA, Jakobs S. Snap-, CLIP- and Halo-Tag Labelling of Budding Yeast Cells. Plos One. 2013; 8:e7874.
37. Bayles AR, Chahal HS, Chahal DS, Goldbeck CP, Cohen BE, Helms BA. Rapid Cytosolic Delivery of Luminescent Nanocrystals in Live Cells with Endosome-Disrupting Polymer Colloids. Nano Lett. 2010; 10:4086–4092. [PubMed: 20831181]
38. Clancy BE, Behnke-Parks WM, Andreasson JO, Rosenfeld SS, Block SM. A universal pathway for kinesin stepping. NaT Struct Mol Bio. 2011; 18:1020–1027. [PubMed: 21841789]
39. Han HS, Devaraj NK, Lee J, Hilderbrand SA, Weissleder R, Bawendi MG. Development of a Bioorthogonal and Highly Efficient Conjugation Method for Quantum Dots Using Tetrazine-Norbornene Cycloaddition. J Am Chem Soc. 2010; 132:7838–7839. [PubMed: 20481508]
40. Shen HY, Jawaid AM, Snee PT. Poly(ethylene glycol) Carbodiimide Coupling Reagents for the Biological and Chemical Functionalization of Water-Soluble Nanoparticles. ACS Nano. 2009; 3(4):915–923. [PubMed: 19275175]
41. Prifti E, Reymond L, Umebayashi M, Hovius R, Riezman H, Johnsson K. A Fluorogenic Probe for SNAP-Tagged Plasma Membrane Proteins Based on the Solvatochromic Molecule Nile Red. ACS Chem Biol. 2014; 9:606–612. [PubMed: 24471525]

42. Sun XL, Zhang AH, Baker B, Sun L, Howard A, Buswell J, Maurel D, Masharina A, Johnsson K, Noren CJ, Xu MQ, Correa IR. Development of SNAP-Tag Fluorogenic Probes for Wash-Free Fluorescence Imaging. Chembiochem. 2011; 12:2217–2226. [PubMed: 21793150]

43. DeWitt MA, Chang AY, Combs PA, Yildiz A. Cytoplasmic Dynein Moves Through Uncoordinated Stepping of the AAA+ Ring Domains. Science. 2012; 335:221–225. [PubMed: 22157083]

44. Sukhanova A, Even-Desrumeaux K, Kisserli A, Tabary T, Reveil B, Millot JM, Chames P, Baty D, Artemyev M, Oleinikov V, Pluot M, Cohen JHM, Nabiev I. Oriented Conjugates of Single-Domain Antibodies and Quantum Dots: Toward a New Generation of Ultrasmall Diagnostic Nanoprobes. Nanomed-Nanotechnol. 2012; 8:516–525.

45. Montenegro JM, Grazu V, Sukhanova A, Agarwal S, de la Fuente JM, Nabiev I, Greiner A, Parak WJ. Controlled Antibody/(Bio-) Conjugation of Inorganic Nanoparticles for Targeted Delivery. Adv Drug Del Rev. 2013; 65:677–688.

46. Petershans A, Wedlich D, Fruk L. Bioconjugation of CdSe/ZnS Nanoparticles with SNAP Tagged Proteins. Chem Comm. 2011; 47:10671–10673. [PubMed: 21887421]

47. Han G, Mokari T, Ajo-Franklin C, Cohen BE. Caged Quantum Dots. J Am Chem Soc. 2008; 130:15811–15814. [PubMed: 18983148]

48. Aldana J, Wang YA, Peng XG. Photochemical Instability of CdSe Nanocrystals Coated by Hydrophilic Thiols. J Am Chem Soc. 2001; 123:8844–8850. [PubMed: 11535092]

49. Zhang ZY, Kenny SJ, Hauser M, Li W, Xu K. Ultrahigh-Throughput Single-Molecule Spectroscopy and Spectrally Resolved Super-Resolution Microscopy. Nat Methods. 2015; 12:935–938. [PubMed: 26280329]

50. Cleary FB, Dewitt MA, Bilyard T, Htet ZM, Belyy V, Chan DD, Chang AY, Yildiz A. Tension on the Linker Gates the ATP-Dependent Release of Dynein from Microtubules. Nat Comm. 2014; 5:4587.

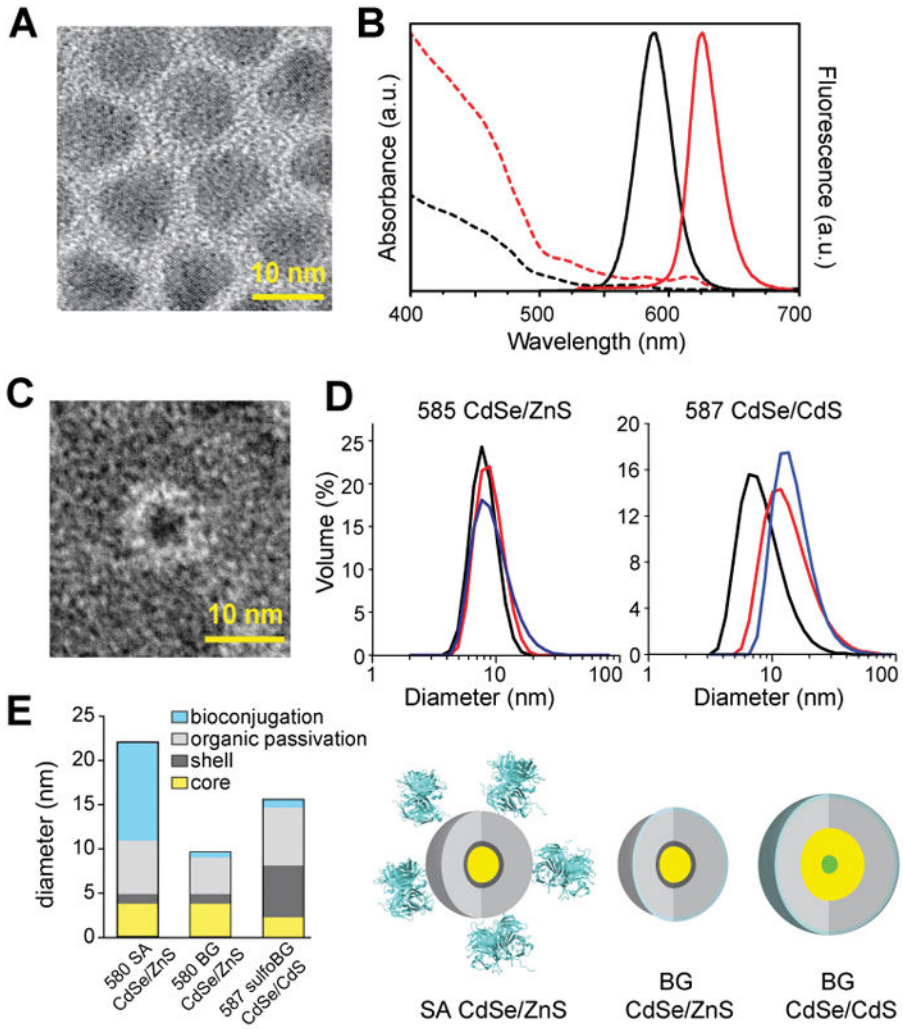

Figure 1.

QD synthesis, and characterization. (*A*) TEM of core/shell CdSe/CdS QDs with 626 nm emission peak. (*B*) Absorption (dotted lines) and emission (solid lines) spectra of CdSe/CdS QDs with 587 nm and 626 nm emission peaks. (*C*) Negative-stain EM image of BG CdSe/ZnS QD with 585 nm emission peak. (*D*) Dynamic light scattering sizing of hydrophobic (black), aqueous (red), and BG-functionalized (blue) 585-nm CdSe/ZnS and 587-nm CdSe/CdS QDs. (*E*) To-scale diameters of SA-coated CdSe/ZnS QDs, and BG-functionalized QDs with emission maxima of ~585 nm, determined by experiment or calculation detailed in Table S1.

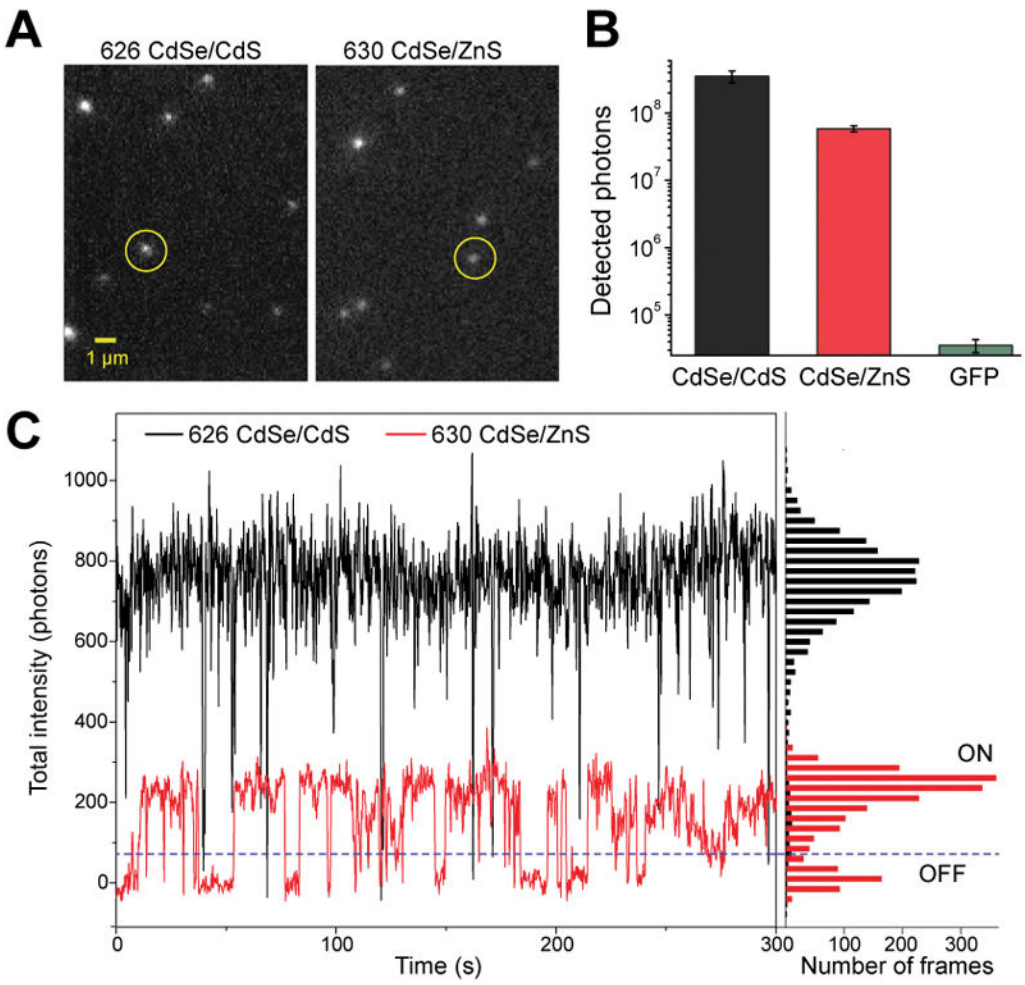

Figure 2.

Single-molecule characterization of CdSe/CdS QDs. (*A*) Individual 630-nm CdSe/CdS QDs (left) and 630 nm CdSe/ZnS QDs (right) under 35 W/cm^2 488-nm TIRF illumination. Yellow circles correspond to the spots plotted in C. (*B*) Total photons collected before photobleaching from single 626 nm CdSe/CdS, 630 nm CdSe/ZnS QDs, and GFP (mean ± SEM; N = 24, 23, and 46, respectively). (*C*) Fluorescence traces of 626-nm CdSe/CdS and 630-nm CdSe/ZnS QDs showing on-off blinking, with histogram showing 99% and 72% of time spent in the on state, respectively.

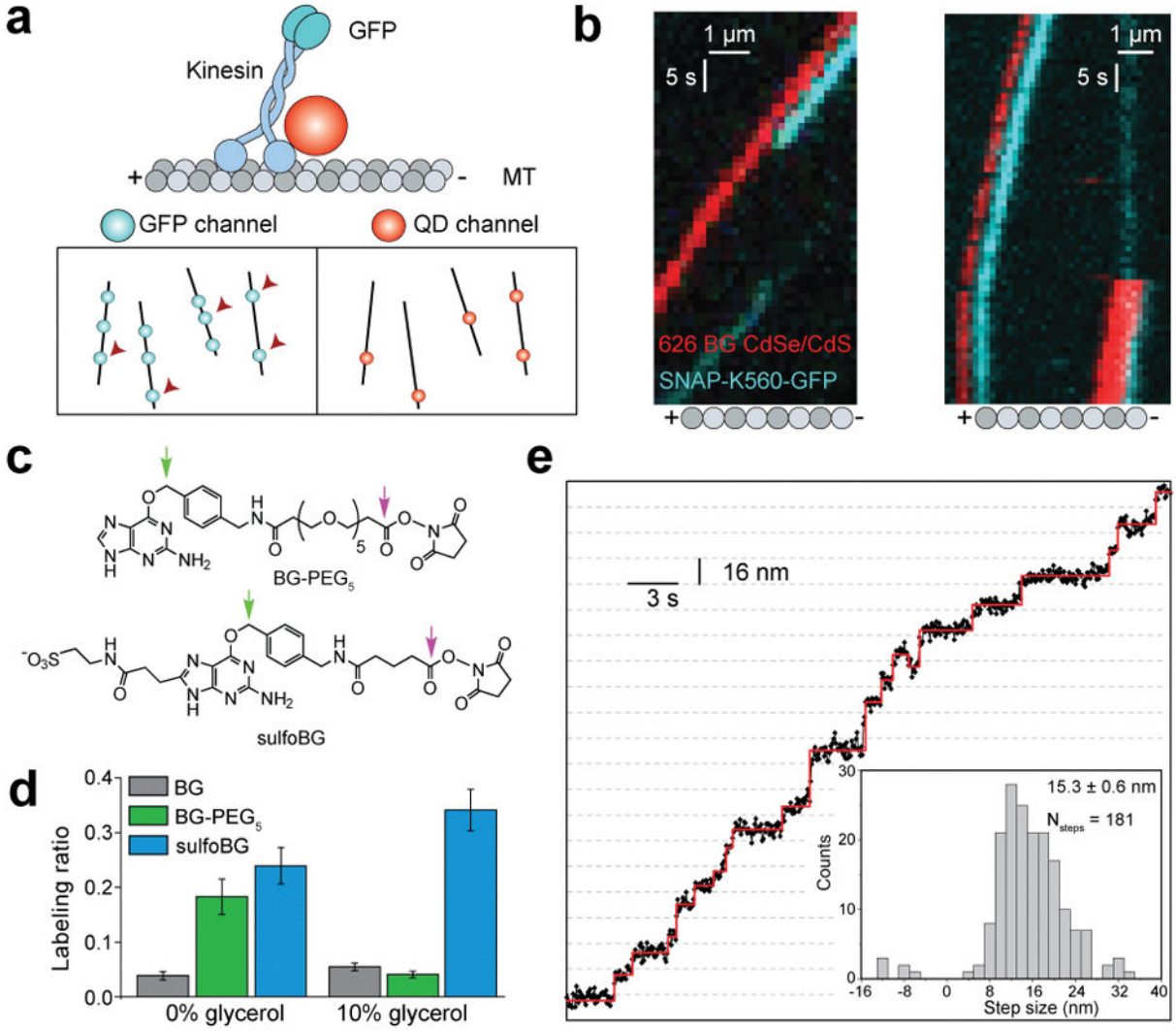

Figure 3.

Improved labeling of protein targets using modified SNAP tags. (*A*) Schematic of *in vitro* microscopy of kinesin labeled with GFP at its tail and sulfoBG-QD at its head. Fluorescence signal is split into two channels and QD labeled motors (arrowhead) is determined by GFP-QD colocalization. (*B*) Representative kymographs show the processive movement of SNAP-K560-GFP motors labeled with a single color of QD. Labeling efficiency of QDs is calculated from the correlative linear movement of QDs with GFP. (*C*) Chemical structures of BG-PEG_5-SE, and sulfoBG-SE ligands. Green and purple arrows mark SNAP protein and amine-functionalized QD attachment sites, respectively. Syntheses are described in Methods and Figure S5. (*D*) Labeling efficiency of QDs functionalized with different SNAP ligands in the presence and absence of 10% glycerol. Error bars are s.e.m. From left to right, N = 20, 19, 10, 17, 20, 11. (*E*) A representative trace (black) for the processive motility of SNAP-K560-GFP labeled with a 630 nm sulfoBG CdSe/CdS QD at 1 μM ATP. The red line is the fit of the trace to the step finding algorithm (see Methods). Inset shows the histogram of step sizes (mean ± s.e.m.).

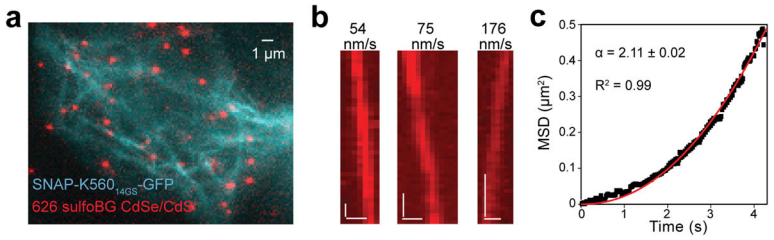

Figure 4.

Live-cell imaging of kinesin using microinjected red sulfoBG QDs. (*A*) TIRF images of HeLa cells expressing SNAP-K560$_{14GS}$-GFP, microinjected with 626-nm sulfoBG CdSe/CdS QDs. K560$_{14GS}$ tightly attaches to microtubules under physiological conditions, illuminating the microtubule network. (*B*) Representative kymographs of QDs that display linear movement inside cells. Vertical scale bars correspond to 2 s elapsed, and horizontal scale bars correspond to 1 μm traveled. (*C*) MSD analysis shows that single QD trajectories represent directed motion, not diffusion (±95% confidence interval).